



Research Article

Semi-Analytical Approach to Analyze the Hull Girder Ultimate Strength Considering the Influence of Side Hopper

Muhammad Zubair Muis Alie^{1*}, Ahmad Fauzan Zakki², Dony Setyawan³, Tuswan², Muslimat Fathanah Rasidi⁴, Ocid Mursid⁵

¹Department of Ocean Engineering, Engineering Faculty, Hasanuddin University, Makassar, 92171, Indonesia

²Department of Naval Engineering, Engineering Faculty, Diponegoro University, Semarang, 50275, Indonesia

³Department Faculty of Marine Technology, Institut Technologi Sepuluh Nopember, Surabaya, 60111, Indonesia

⁴Department of Naval Architecture, Engineering Faculty, Hasanuddin University, Makassar, 92171, Indonesia

⁵Department Of Naval Architecture, Ocean and Marine Engineering, University of Strathclyde, Glasgow, G1 1XQ, United Kingdom

*Corresponding author: zubair.m@eng.unhas.ac.id; Tel.: +6281382815767

Abstract: A bilge hopper is one of the sections on ship bottom construction. The side hopper has an angle required in the national classification at the bilge hopper. This angle depends on the type of the ship's hull, whether the ship has a single or double hull construction. This study aims to assess the impact of the side hopper angle at the bilge section on the strength of the ship structure. The bulk carrier and oil tanker are considered as the ship's objects. The cross sections of the bulk carrier and oil tanker are assessed. It is thought that the cross-section of those ships remained plane throughout the gradual collapse. One frame space, measured along the length of the ship from one web frame to another, is considered for basic computations and analysis. The slope angle of the side hopper analysis is based on national classification regulations, which specify a slope angle of 35°. The semi-analytical approach is adopted to evaluate the ultimate ship hull girder strength. In this study, we compare and discuss the results obtained from the ultimate strength considering the influence of side hopper angle for oil tanker and bulk carrier between the existing condition and local classification.

Keywords: Bulk carrier; Cross-section; Oil tanker; Semi-analytical; Ultimate strength

1. Introduction

The ship's bottom structure plays a crucial role in preventing damage, such as grounding or collision. The ship's bottom, located in the middle and especially the bilge, generally has a slope on the hopper's side. This side hopper is connected to the ship's side, depending on whether the ship has a single or double side. A side hopper with this slope is mentioned in the national classification regulations (Biro Klasifikasi Indonesia, 2024), where the slope angle is equal to 35°. Therefore, the 35° slope angle of this side hopper needs to be investigated in relation to the strength of the ship. The influence of the side hopper angle on the strength of the ship is the novelty of this study.

Many studies have analyzed the strength and behavior of ship structures, but none have examined the influence of the side hopper angle on the ultimate hull girder strength of ship structures. Georgiadis et al., 2023 proposed a Bayesian analysis for the probabilistic modeling of X_r , which can be applied for the design and assessment of container ships. Deng et al., 2022 and Zhao et al., 2022 investigated the ultimate strength of a ship hull girder model using nonlinear finite element analysis to consider deck openings. Another type of ship, such as a container with 10000 TEUS, was also analyzed for its collapse behavior using the finite element method (Q. Wang and Wang, 2020; Q. Wang et al., 2020), including the influence of the nonlinear finite

element method model on the ultimate bending moment for the hull girder (Xu et al., 2017). A simple box girder can also be investigated using the finite element method, including its behavior (Song et al., 2025; Y. Wang et al., 2024; Quispe et al., 2022; Bai et al., 2021; Downes et al., 2017). A long-term hydroelastic analysis that looked at the local and lateral loads provided by different cargo loading scenarios resulted in a combined hull-girder bending moment and the dynamic ultimate capacity of ultra-large container ships under realistic loading scenarios. Jagite et al., 2022. Shi and Gao, 2021 carried out a collapse experiment on a steel model with superstructures, which was designed based on an actual cruise ship. S. Li et al., 2021 proposed a probabilistic approach to evaluate the prediction uncertainty of the ultimate strength of the hull girder caused by the critical characteristics within the LSC. The analysis of the ultimate hull girder strength considering the load combination, such as bending moment, lateral pressure, and cyclic loads, has also been discussed (Y. Wang et al., 2025; D. Li et al., 2023; Ma et al., 2022; Campanile et al., 2017). Under cyclic loading, the ship hull girder may have a lower strength than under monotonically rising bending moment, as the standard analysis assumes, as demonstrated by Liu et al., 2020.

By considering the likelihood and effects of a structural failure, risk assessment techniques and principles established an acceptable target reliability range for VLFS. X. Wang and Gu, 2021 developed a reliability evaluation methodology to meet the ultimate strength design standards of VLFS. Furthermore, several researchers have analyzed the ultimate strength of ships, plates, and stiffeners by considering the influence of geometric imperfections, such as Z. Li et al., 2025; Cui et al., 2024; Georgiadis and Samuelides, 2021; Estefen et al., 2016. Corrosion and crack damage on the hull girder has also been analyzed by Feng et al., 2025 and Babazadeh and Khedmati, 2021. Research related to the damage caused by collisions has also been analyzed, some of them are Chen et al., 2022; S. Li and Kim, 2022; Liu et al., 2021; Zhang et al., 2021; Kuznecovs et al., 2020. D. Li and Chen, 2025 proposed a novel strategy mainly involving an equivalent sequential loading approach and an artificial intelligence method. Based on experimental and numerical analysis, Z. Wang et al., 2023 proposed an empirical formula to assess the ultimate strength of the side shell of a passenger ship under combined axial and shear load. Barsotti et al., 2025 developed a blind benchmark in which multiple international research institutions analyzed the same geometry to compare nonlinear numerical modeling approaches adopted in PCA. Zhu et al., 2024 proposed a novel method for determining the neutral axis position of the asymmetric cross-section and its application in the SPC method for damaged ships. Prabu-Chelladurai et al., 2023 developed a method to calculate the instantaneous shear force and bending moment of a ship in waves using point clouds.

Several studies related to structural analysis using finite element methods, such as Design and Analysis of Floater Structures using Composite Material in 19-Seater Aircraft, were conducted by Kadir et al., 2025, where the structure was modeled using the finite element model to reduce the weight of floaters by applying the optimal design and sandwich composite materials. Hamza et al., 2023 used finite element analysis to investigate the effect of the angle of attack on coefficients and forces, particularly on a blade air foil in a horizontal axis wind turbine. The finite element analysis of the lattice structure model with control volume manufactured using additive manufacturing was conducted by Kholil et al., 2023. Akbar et al., 2022 presented a new insight on the potential of piezo aeroelastic energy harvesting on the transport aircraft wing structure, where the numerical method in terms of finite element analysis was adopted.

According to a previous study, this study proposes a new investigation on the side hopper angle at the bilge to the ultimate hull girder strength.

2. Methods

The material data and methods are presented in Sections 2.1 and 2.2, respectively.

2.1 Material data

In this study, the bilge-side hopper structure is based on the national classification rules (Biro Klasifikasi Indonesia). Figure 1 shows the hopper side scheme adopted from the Biro Klasifikasi Indonesia, 2024, which serves as a reference in determining the geometry of the analyzed hopper side. The hopper side structure illustrates the relationship between the inner bottom and inner hull, with a slope angle of 35° applied in accordance with national standards.

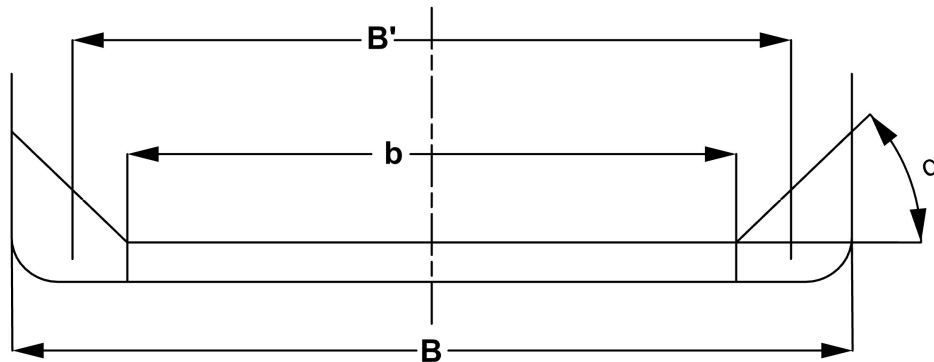


Figure 1 Side hopper angle at the bilge part adopted from Biro Klasifikasi Indonesia, 2024

The material characteristics of the oil tanker and bulk carrier, such as density, yield strength, Poisson's ratio, and Young's modulus, are shown in Table 1. Two oil tankers (T3 and T4) and one bulk carrier (B1) are used for analysis, as shown in Table 2. The difference between the two oil tankers is based on the type and dimensions of the stiffened plates. The analysis excludes considerations of initial deflection, corrosion, and cracks. It is assumed that the cross-section remains plane during progressive collapse assessment. For simple calculation and analysis, a single frame space is considered for both oil tankers and bulk carriers. For oil tankers, one frame space is equal to 5 m, whereas for bulk carriers, one frame space is equal to 4.175 m. All elements that support the ship's longitudinal strength are included in the analysis. The cross sections of the oil tankers (T3 and T4) and bulk carrier (B1) are illustrated in Figure 2.

Table 1 Material properties

| Items | Value | Unit |
|----------------|--------------------|-------------------|
| Density | 7850 | kg/m ³ |
| Young Modulus | 2×10^{11} | N/mm ² |
| Poisson Ratio | 0.3 | - |
| Yield Strength | 315/355 | MPa |

Table 2 Ship dimensions (m)

| Ship | B1 | T3 | T4 |
|-------|--------|------|------|
| L (m) | 217 | 234 | 234 |
| B (m) | 32.236 | 44 | 44 |
| D (m) | 18.3 | 21.2 | 21.2 |

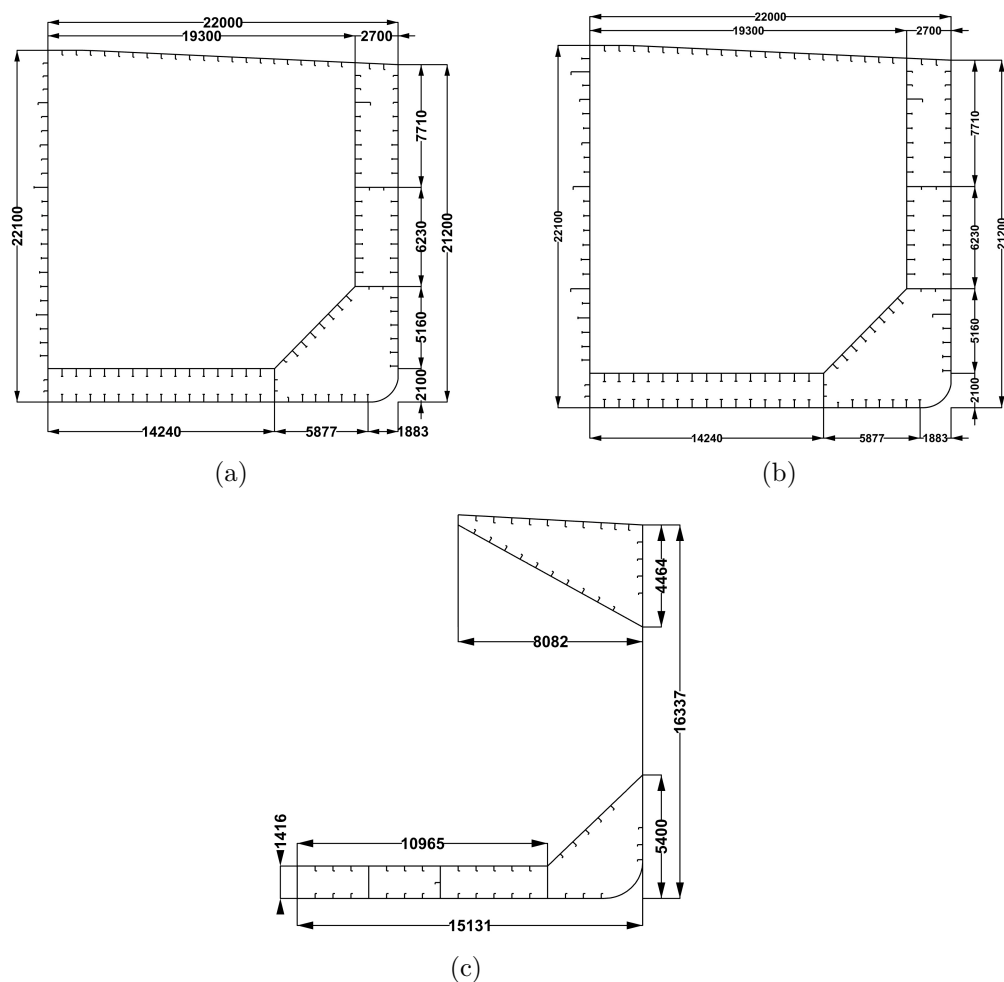


Figure 2 Cross-Section of Oil Tanker and Bulk Carrier in (mm) (a) Oil Tanker (T3) (b) Oil Tanker (T4) (c) Bulk Carrier (B1)

2.2 Analysis Procedure

This study examines how the side hopper angle influences the ultimate strength using semi-analytical techniques. The cross-section of bulk carriers and oil tankers under hogging and sagging situations is analyzed while considering the side hopper angle. By applying Smith's technique to the software code HULLST created by Yao and Nikolov, 1992, the strength of two oil tankers and one bulk carrier is examined using a semi-analytical methodology. The general procedure for the analysis may be described as follows:

1. The cross-section, as in Zhao et al., 2022 into elements composed of stiffener and attached plating, as shown in Figure 3 for the oil tanker and bulk carrier, together with and without changing the side hopper angle of 45° and 35° at the bilge part for the oil tanker and bulk carrier, as shown in Figure 4. In the side hopper part, the slope of 45° was changed to 35° according to the regulation of Biro Klasifikasi Indonesia, 2024. In addition, a stiffener has been moved to the inner hull section due to the amount of stiffener located at the side hopper; however, this is only for oil tankers. For a bulk carrier, the stiffener is not moved because the ship does not have an inner hull. In addition, the number of stiffeners in the side hopper part on bulk carriers is quite small, which differs from that of oil tankers. Variables a, b, c, and d, which are the stiffener dimensions and types, correspond to Figure 3 for the oil tanker and bulk carrier. It should be noted that type T3 and T4 oil tankers have the same dimensions except for the stiffener dimensions and types.

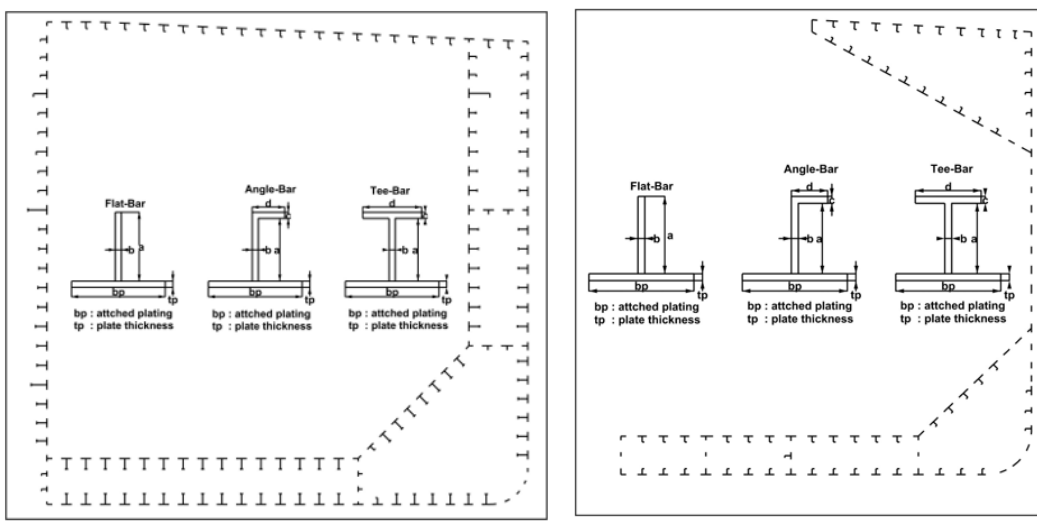


Figure 3 Subdivision into plates and stiffeners of Oil Tanker and Bulk Carrier cross-section
 (a) Oil Tanker (b) Bulk Carrier

2. Calculate each element's average stress-average strain relationships using Equation 1, taking yielding and buckling into account.

$$\sigma = f_i(\varepsilon) \quad (1)$$

3. Using the average stress-average strain curve at the current strain, the tangential axial stiffness of each individual element D_i , Equation 2.

$$\Delta\sigma = D_i \Delta\varepsilon \quad \text{with} \quad D_i = \left(\frac{df_i}{d\varepsilon} \right) \quad (2)$$

4. The centroidal position of the instantaneous neutral axis, Y_G and Z_G , is determined using Eqs. (3) and (4).

$$Y_G = \frac{\sum_{i=1}^N Y_i D_i A_i}{\sum_{i=1}^N D_i A_i} \quad (3)$$

$$Z_G = \frac{\sum_{i=1}^N Z_i D_i A_i}{\sum_{i=1}^N D_i A_i} \quad (4)$$

5. Using Eqs. (5) and (6), the flexural stiffness of the cross-section is determined with respect to the instantaneous neutral axis.

$$\begin{Bmatrix} \Delta M_H \\ \Delta M_V \end{Bmatrix} = \begin{bmatrix} D_{HH} & D_{HV} \\ D_{VH} & D_{VV} \end{bmatrix} \begin{Bmatrix} \Delta\phi_H \\ \Delta\phi_V \end{Bmatrix} \quad (5)$$

$$\begin{aligned}
D_{AA} &= \sum_{i=1}^N D_i A_i \\
D_{HV} = D_{VH} &= - \sum_{i=1}^N D_i (Y_i - Y_G)(Z_i - Z_G) A_i \\
D_{HH} &= \sum_{i=1}^N D_i (Y_i - Y_G)^2 A_i \\
D_{VV} &= \sum_{i=1}^N D_i (Z_i - Z_G)^2 A_i
\end{aligned} \tag{6}$$

6. The unknown increments of curvature and/or bending moment under the specified condition are calculated using Equations 7 and 8.

The residual strength analysis of a hull girder under the following loading and restriction conditions can be performed using Equation 5, which is the incremental version of the bending moment-curvature relationship. For this analysis, the hull girder is taken under pure vertical bending moment. The vertical curvature ϕ_V is increased under the condition of $M_H = 0$.

$$\begin{Bmatrix} 0 \\ \Delta M_V \end{Bmatrix} = \begin{bmatrix} D_{HH} & D_{HV} \\ D_{VH} & D_{VV} \end{bmatrix} \begin{Bmatrix} \Delta \phi_H \\ \Delta \phi_V^0 \end{Bmatrix} \tag{7}$$

The superscript “0” denotes a predefined value. The solutions are

$$\Delta \phi_H = - \frac{D_{HV}}{D_{HH}} \Delta \phi_V^0, \quad \Delta M_V = \left(D_{VV} - \frac{D_{VH} D_{HV}}{D_{HH}} \right) \Delta \phi_V^0 \tag{8}$$

$\Delta \phi_H$ indicates that the horizontal curvature is induced by the vertical bending moment when the damage is at asymmetric positions. The residual strength is calculated from the peak value of the $M_V - \phi_V$ curve.

7. Using the slope of the average stress-average strain curve, the strain increments in each individual element are determined based on the curvature increment.

8. Equations 9 and 10 should be added to the cumulative values of the elements to reflect the obtained increases in curvature, bending moment, strains, and stresses.

$$\varepsilon_i(y_i, z_i) = \varepsilon_0 + y_i \phi_H + z_i \phi_V \tag{9}$$

$$\begin{aligned}
P^{n+1} &= P^n + \Delta P & P^{n+1} &= P^n + \Delta P \\
M_H^{n+1} &= M_H^n + \Delta M_H & \phi_H^{n+1} &= \phi_H^n + \Delta \phi_H \\
M_V^{n+1} &= M_V^n + \Delta M_V & \phi_V^{n+1} &= \phi_V^n + \Delta \phi_V
\end{aligned} \tag{10}$$

9. The position of the neutral axis for the cumulative values of stress and strain, Equation 11.

$$\varepsilon_0 + y \phi_H + z \phi_V = 0 \tag{11}$$

10. Proceed to the next step.

3. Results and Discussion

Figure 4 shows the changes in the side hopper slope angle of the bilge area for oil tankers and bulk carriers. These slope changes are based on the 2024 regulations of Biro Klasifikasi Indonesia, 2024, which stipulate a side hopper slope angle of 35° . The current slope angle for oil tankers and bulk carriers is 45° . The analysis is performed for slope angles of 45° and 35° . This study examines the strength of bulk carriers and oil tankers while considering the impact of the side hopper angle under drooping and hogging conditions. The port and starboard cross-sections of oil tankers and bulk carriers are symmetrical; therefore, only half of the cross-section is shown in Figure 4. The oil tanker cross section is almost like a box hull girder, with an inner hull (double shell) and a double bottom. Unlike a bulk carrier, even though the ship has a double bottom, the side shell is single. Moreover, a bulk carrier has two tanks, namely, a bilge hopper and a top-side tank, and a hatch that functions to enter and remove goods from the inside cargo hold, as shown in Figure 4.

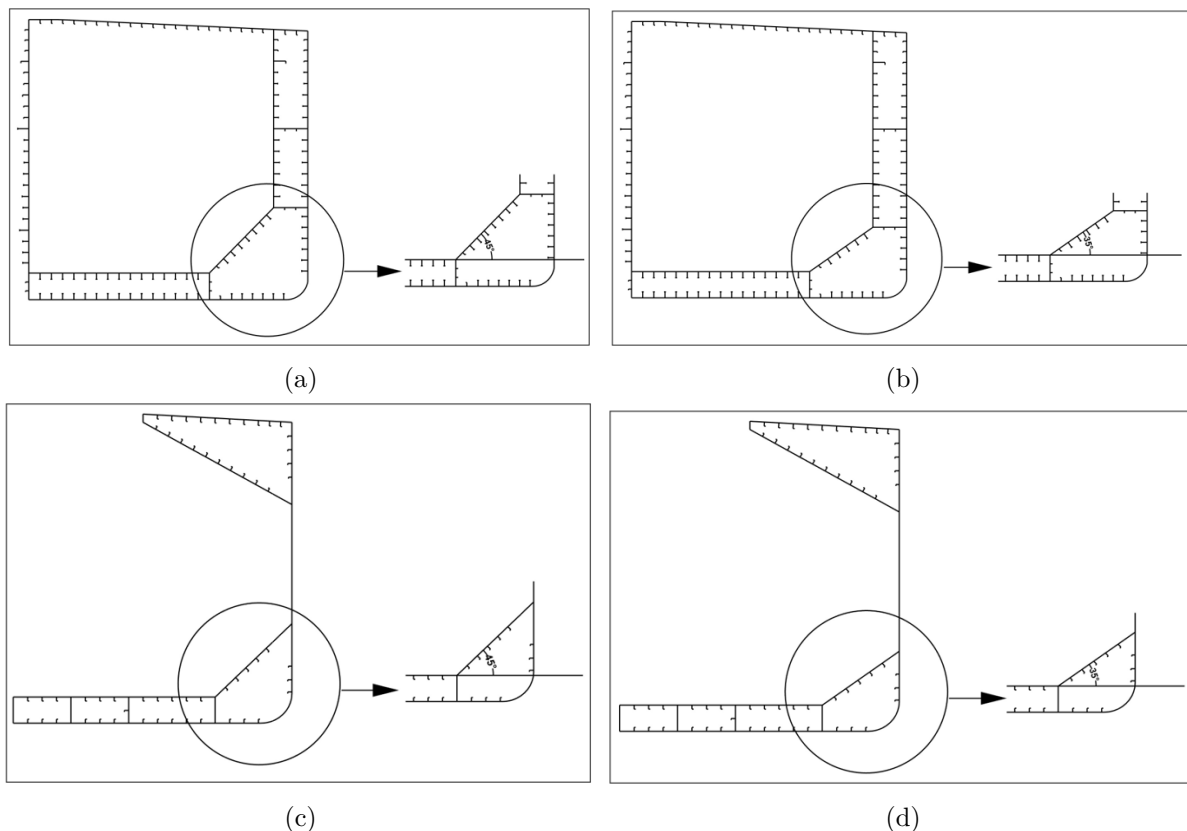


Figure 4 Side hopper angle of Oil Tanker and Bulk Carrier (a) Oil Tanker 45° (b) Oil tanker 35° C (c) Bulk carrier 45° (d) Bulk carrier 35°

Most of the ship hull girder ultimate strength analysis results are in the form of moment-curvature/rotation/displacement, reaction force versus displacement, stress-strain, curves for example as described by other researchers (Barsotti et al., 2025; Cui et al., 2024; Chen et al., 2022; Babazadeh and Khedmati, 2021). The ultimate strength is described in terms of the moment-curvature relationships for oil tankers T3 and T4 at 45° and 35° angles under hogging and sagging conditions, as shown in Figures 5 (a) and 5 (b). Meanwhile, the moment-curvature relationship for a bulk carrier at 45 degrees and 35 degrees angle under hogging and sagging conditions is illustrated in Figure 5 (c). It is a minor value according to the oil tanker T3 and T4 moment-curvature relationship curve at 45 degrees and 35 degrees angles under hogging and sagging load situations (Figures 5 (a) and 5 (b)). This is because of the presence of an inner hull on the oil tanker. Although a stiffener is moved from the side hopper to the inner hull, and this side hopper forms a 35° angle, its influence is small at around 0.69% and 0.022% under hogging and sagging conditions, respectively, for oil tanker T3. In the case of oil tanker T4,

the difference is 0.45% in the hogging condition and 0% in the sagging condition. Furthermore, for the bulk carrier, the difference is 2.24% in the hogging condition and 2.19% in the sagging condition. There are differences in the moment-curvature curve results for bulk carrier ships because the bulk carrier only has a single hull. In addition, the stiffener position does not change because the number of stiffeners in the side hopper is relatively small. Therefore, the angle of the side hopper influences the strength. The results of the differences in the moment-curvature relationship at 45 and 35 degrees under hogging and sagging conditions for the three ships are summarized in Table 3. The inertia and the position of the neutral axis also experienced changes caused by the angle of the side hopper on oil tankers and bulk carriers. The most visible effect is captured on bulk carriers and the smallest effect is captured on oil tankers. Table 4 summarizes the inertia and the neutral axis.

Table 3 Ultimate strength of Oil Tankers and Bulk Carriers

| Ship Types | Ultimate Hogging Moment (M_{UH}) $\times 10^{12}$ Nmm | Ultimate Sagging Moment (M_{US}) $\times 10^{12}$ Nmm |
|----------------------------|--|--|
| Oil Tanker T3 (45 Degrees) | 1.3000 | -0.9298 |
| Oil Tanker T3 (35 Degrees) | 1.3090 | -0.9300 |
| Oil Tanker T4 (45 Degrees) | 1.5370 | -1.1450 |
| Oil Tanker T4 (35 Degrees) | 1.5440 | -1.1450 |
| Bulk Carrier (45 Degrees) | 6.7790 | -5.9750 |
| Bulk Carrier (35 Degrees) | 6.6270 | -6.1090 |

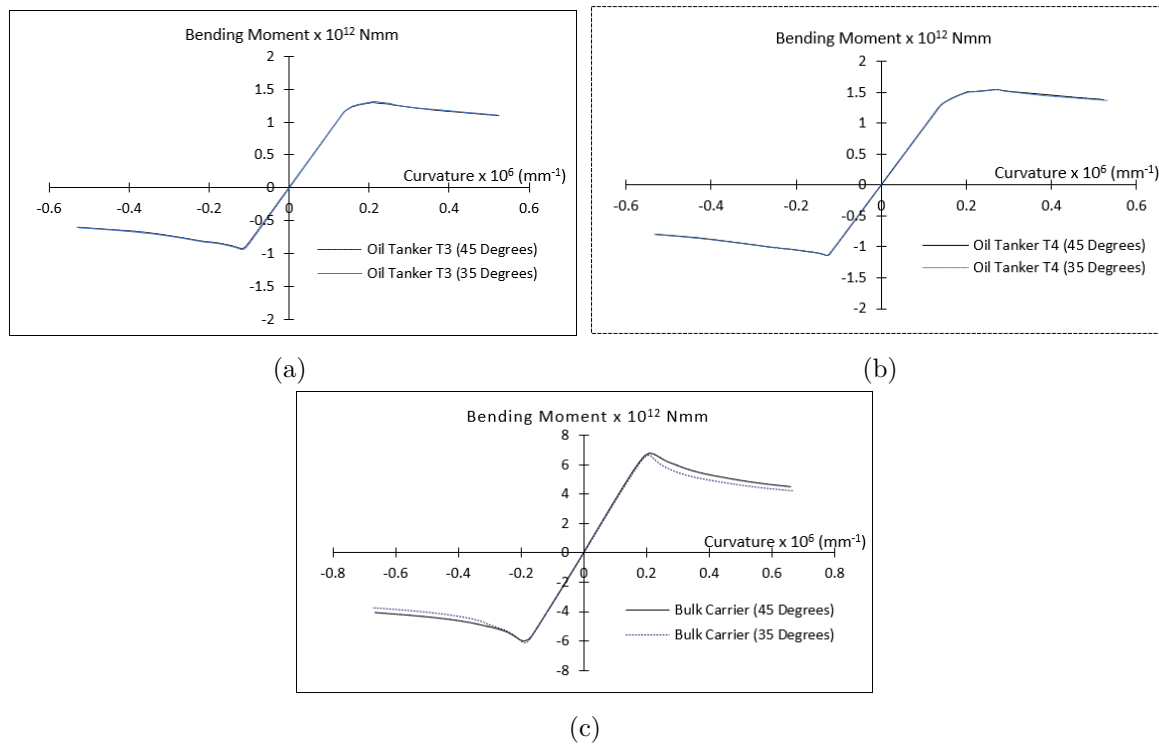


Figure 5 Moment-Curvature Relationship (a) Oil Tanker (T3) (b) Oil Tanker (T4) (c) Bulk carrier

The stress distribution on two oil tankers (T3) (Figures 6 (a) and (b)) and (T4) (Figures 6 (c) and (d)) and a bulk carrier (Figures 6 (e) and (f)) with side hopper angles of 45° and 35°. According to Figure 6, the red triangles indicate that parts of the ships are in compression (yielding), while the blue circles indicate that the parts are buckling when it takes place, and vice versa. Buckling and yielding may occur on the ship when it is under hogging or sagging

conditions. The figure shows that the influence of the side hopper on the bulk carrier may appear because it does not have the double-sided structure, unlike oil tankers. Figure 6 also shows that the stress distributions on the deck and bottom for oil tankers with 45° and 35° side hopper angles are approximately identical (the difference is quite small). However, on bulk carriers, there is a difference, where the elements located at the deck part yielding slightly take place with a 35° side hopper angle of 35° rather than 45° .

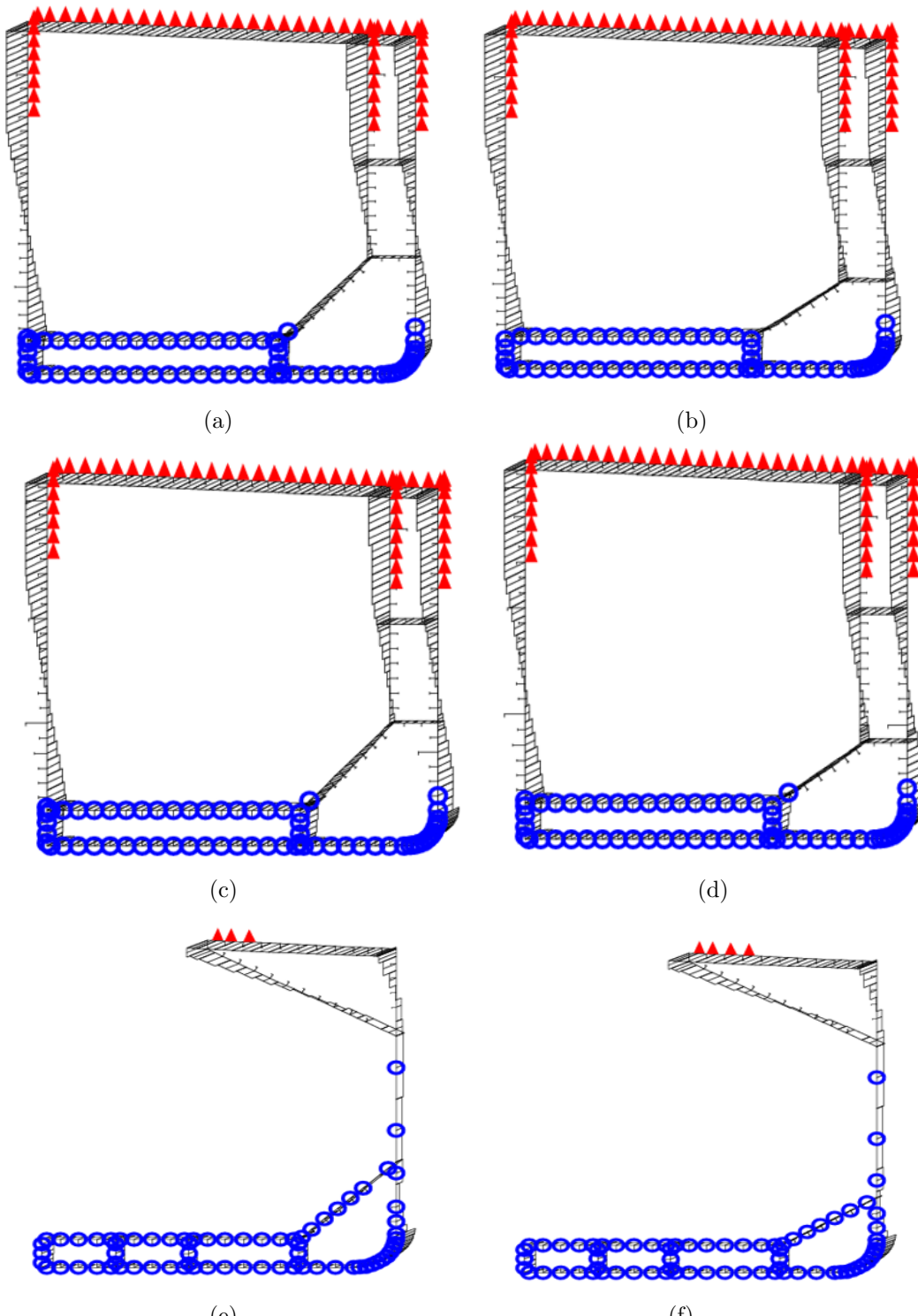


Figure 6 Stress distributions and failure modes of oil tankers and bulk carriers (a) Oil tanker (T3) at 45° (b) Oil tanker (T3) at 35° (c) Oil tanker (T4) at 45° (d) Oil tanker (T4) at 35° (e) Bulk carrier with 45° (f) Bulk carrier with 35°

As explained in the introduction, no research has been conducted on the strength of ship structure considering the influence of side hopper angle on both oil tankers and bulk carriers. The bulk carrier studied by Babazadeh and Khedmati, 2021 was also analyzed to determine the ultimate strength of the ship; however, the focus was on the influence of cracks on the outer bottom, inner bottom, side shell, and deck structures. This bulk carrier ship has also been extensively analyzed by other researchers, but the problem of the side hopper angle has not yet been addressed. Similar to oil tankers, although many researchers have analyzed the strength of these tankers, the influence of the side hopper angle has not been considered. Deng et al., 2022 conducted the ultimate strength analysis of the box girder only on the deck, considering large openings. Similarly, Zhao et al., 2022 considered large openings on the ship's deck. Both studies used experimental and numerical methods. The Nonlinear Finite Element code of Abaqus and LS-Dyna software are used for modeling and numerical analysis. The experimental and numerical results were then compared. Although those studies are the most similar to the current one, they did not consider how the angle of the side hoppers affected the ultimate hull girder strength. This study focuses on the investigation and creation of national regulations of shipbuilding.

Table 4 Inertia and neutral axis

| Ship Types | Inertia $\times 10^{15}$ (mm ⁴) | Neutral Axis (mm) |
|---------------------------------|---|-------------------|
| Oil Tanker (T3) with 45 Degrees | 1.340 | 0.889 |
| Oil Tanker (T3) with 35 Degrees | 1.360 | 0.884 |
| Oil Tanker (T4) with 45 Degrees | 1.400 | 0.909 |
| Oil Tanker (T4) with 35 Degrees | 1.420 | 0.904 |
| Bulk Carrier with 45 Degrees | 0.421 | 0.850 |
| Bulk Carrier with 35 Degrees | 0.417 | 0.840 |

4. Conclusions

This study used a semi-analytical method to evaluate the strength of two oil tankers and a bulk carrier, considering the side hopper angle at the bilge part. The cross-section of both ships is investigated. Subsequently, the ultimate strength of oil tankers and bulk carriers is compared with and without changing the side hopper angle at the bilge part. The effect of the angle on the ship's strength in the side hopper of oil tankers is quite small, due to the presence of an inner hull. On bulk carriers, there is a difference in stress distribution, with elements experiencing slightly more yielding on the deck area at a side hopper angle of 35° compared to 45°. The results obtained from the moment-curvature relationship indicate that the side hopper angle affects the ultimate strength of the ship with a uniform stress distribution on oil tankers due to their intact cross-sectional shape without any openings. However, this is not the case for bulk carriers with hatches.

Acknowledgements

The author declares that the Research Collaboration Program funded this research through a research contract number 01319/UN4.22/PT.01.03/2025. The author also stated that Grammarly and QuillBot are used to check grammatical errors and Paraphrasing Tool.

Author Contributions

Muhammad Zubair Muis Alie: Writing – original draft, Review & editing, Visualization, Validation, Calculation procedure, Project administration, Methodology, Investigation, Formal analysis, Data curation, Conceptualization. Ahmad Fauzan Zakki: Review & editing, Validation, Supervision, Resources, Project administration, Funding acquisition, Conceptualization.

Dony Setyawan: Review & editing, Validation, Supervision, Resources, Methodology, Investigation. Tuswan: Review & editing, Validation, Supervision, Resources, Project administration, Funding acquisition, Conceptualization. Muslimat Fathanah Rasidi: Review & editing, Visualization, Validation, Calculation procedure, Investigation, Formal analysis, Data analysis. Ocid Mursid: Review & editing, Visualization, Investigation, Supervision.

Conflict of Interest

The authors declare that they have no known competing financial interests or personal relationships that could have influenced the work reported in this paper.

Supplementary Materials

Supplementary material has been included in the article.

References

Akbar, M., Ramadhan, M. J., Izzuddin, M., Gunawan, L., Sasongko, R. A., Kusni, M., & Curiel-Sosa, J. L. (2022). Evaluation of piezoaeroelastic energy harvesting potential of a jet transport aircraft wing with multiphase composite using iterative finite element method. *International Journal of Technology*, 13(4), 803–815. <https://doi.org/10.14716/ijtech.v13i4.5468>

Babazadeh, A., & Khedmati, M. R. (2021). Progressive collapse analysis of a bulk carrier hull girder under longitudinal vertical bending moment considering cracking damage. *Ocean Engineering*, 242, 110140. <https://doi.org/10.1016/j.oceaneng.2021.110140>

Bai, L., Shen, R., Yan, Q., Wang, L., Miao, R., & Zhao, Y. (2021). Progressive-models method for evaluating interactive stability of steel box girders for bridges– extension of progressive collapse method in ship structures. *Structures*, 33, 3848–3861. <https://doi.org/10.1016/j.istruc.2021.06.061>

Barsotti, B., Battini, C., Gaiotti, M., Rizzo, C. M., & Vergassola, G. (2025). Experimental and numerical assessment of ultimate strength of a transversally loaded thin-walled deck structure. *Marine Structures*, 103, 103793. <https://doi.org/10.1016/j.marstruc.2025.103793>

Biro Klasifikasi Indonesia. (2024). Rules for hull 2024.

Campanile, A., Piscopo, V., & Scamardella, A. (2017). Incidence of load combination methods on time-variant oil tanker reliability in intact conditions. *Ocean Engineering*, 130, 371–384. <https://doi.org/10.1016/j.oceaneng.2016.12.005>

Chen, B.-Q., Liu, B., & Guedes-Soares, C. (2022). Experimental and numerical investigation on a double hull structure subject to collision. *Ocean Engineering*, 256, 111437. <https://doi.org/https://doi.org/10.1016/j.oceaneng.2022.111437>

Cui, H., Hu, R., Chen, Z., & Zheng, C. (2024). Research on ultimate strength of hull girder considering initial imperfections under monotonic and cyclic bending moments- a bulk carrier case. *Ocean Engineering*, 311, 118862. <https://doi.org/10.1016/j.oceaneng.2024.118862>

Deng, H., Yuan, T., Gan, J., Liu, B., & Wu, W. (2022). Experimental and numerical investigations on the collapse behaviour of box type hull girder subjected to cyclic ultimate bending moment. *Thin-Walled Structures*, 175, 109204. <https://doi.org/https://doi.org/10.1016/j.tws.2022.109204>

Downes, J., Tayyar, G., Kvan, I., & Choung, J. (2017). A new procedure for load-shortening and elongation data for progressive collapse method. *International Journal of Naval Architecture and Ocean Engineering*, 9(6), 705–719. <https://doi.org/10.1016/j.ijnaoe.2016.10.005>

Estefen, S. F., Chujutalli, J. H., & Guedes-Soares, C. (2016). Influence of geometric imperfections on the ultimate strength of the double bottom of a suezmax tanker. *Engineering Structures*, 127, 287–303. <https://doi.org/https://doi.org/10.1016/j.engstruct.2016.08.036>

Feng, L., Ai, F., Wang, C., Yu, J., & Cui, Z. (2025). Residual ultimate strength of hull plates under irregular pitting corrosion: An innovative numerical simulation approach and experimental validation. *Ocean Engineering*, 318, 120092. <https://doi.org/https://doi.org/10.1016/j.oceaneng.2024.120092>

Georgiadis, D. G., & Samuelides, M. S. (2021). Stochastic geometric imperfections of plate elements and their impact on the probabilistic ultimate strength assessment of plates and hull-girders. *Marine Structures*, 76, 102920. <https://doi.org/10.1016/j.marstruc.2020.102920>

Georgiadis, D., Samuelides, E., & Straub, D. (2023). A bayesian analysis for the quantification of strength model uncertainty factor of ship structures in ultimate limit state. *Marine Structures*, 92, 103495. <https://doi.org/10.1016/j.marstruc.2023.103495>

Hamza, S., Ahmadizadeh, M., Dashtizadeh, M., & Chitt, M. (2023). Modification of horizontal wind turbine blade: A finite element analysis. *International Journal of Technology*, 14(1), 5–14. <https://doi.org/10.14716/ijtech.v14i1.5255>

Jagite, G., Bigot, F., Malenica, S., Derbanne, Q., Sourne, H. L., & Cartraud, P. (2022). Dynamic ultimate strength of an ultra-large container ship subjected to realistic loading scenarios. *Marine Structures*, 84, 103197. <https://doi.org/https://doi.org/10.1016/j.marstruc.2022.103197>

Kadir, A. M., Setyawan, A., Purnamasari, F. N., Pramana, N., Muhammad, Satriya, I. A. A., Wirawan, R., & Sampurno, B. (2025). Design and analysis of floater structures using composite material in 19 seaters aircraft. *International Journal of Technology*, 16(1), 112–123. <https://doi.org/https://doi.org/10.14716/ijtech.v16i1.6326>

Kholil, A., Kiswanto, G., Al Farisi, A., & Istiyanto, J. (2023). Finite element analysis of lattice structure model with control volume manufactured using additive manufacturing. *International Journal of Technology*, 14(7), 1428–1437. <https://doi.org/https://doi.org/10.14716/ijtech.v14i7.6660>

Kuznecovs, A., Ringsberg, J. W., Johnson, E., & Y, Y. (2020). Ultimate limit state analysis of a double-hull tanker subjected to biaxial bending in intact and collision-damaged conditions. *Ocean Engineering*, 209, 107519. <https://doi.org/10.1016/j.oceaneng.2020.107519>

Li, D., & Chen, Z. (2025). Generalized closed-form formulae for characterizing the ultimate strength envelope of ship stiffened panels subjected to combined biaxial compression and lateral pressure. *Marine Structures*, 102, 103789. <https://doi.org/https://doi.org/10.1016/j.marstruc.2025.103789>

Li, D., Chen, Z., & Chen, X. (2023). Numerical investigation on the ultimate strength behaviour and assessment of continuous hull plate under combined biaxial cyclic loads and lateral pressure. *Marine Structures*, 89, 103408. <https://doi.org/https://doi.org/10.1016/j.marstruc.2023.103408>

Li, S., & Kim, D. K. (2022). A comparison of numerical methods for damage index based residual ultimate limit state assessment of grounded ship hulls. *Thin-Walled Structures*, 172, 108854. <https://doi.org/https://doi.org/10.1016/j.tws.2021.108854>

Li, S., Kim, D. K., & Benson, S. (2021). A probabilistic approach to assess the computational uncertainty of ultimate strength of hull girders. *Reliability Engineering and System Safety*, 213, 107688. <https://doi.org/https://doi.org/10.1016/j.ress.2021.107688>

Li, Z., Lan, S., Xia, T., & Cui, H. (2025). Ultimate strength research on a container ship under pure bending, torsion and bending-torsion combination considering initial imperfections. *Ocean Engineering*, 326, 120783. <https://doi.org/https://doi.org/10.1016/j.oceaneng.2025.120783>

Liu, B., Villavicencio, R., Pedersen, P. T., & Soares, C. G. (2020). Ultimate strength assessment of ship hull structures subjected to cyclic bending moments. *Ocean Engineering*, 215, 107685. <https://doi.org/10.1016/j.oceaneng.2020.107685>

Liu, B., Zhang, H., Wang, Y., & Guedes Soares, C. (2021). Analysis of structural crashworthiness of double-hull ships in collision and grounding. *Marine Structures*, 76, 102898. <https://doi.org/10.1016/j.marstruc.2020.102898>

Ma, H., Wang, Q., & Wang, D. (2022). Scaling characteristics of the hull girder's ultimate strength subjected to the combined hogging moment and bottom lateral pressure: An empirically modified scaling criterion. *Ocean Engineering*, 257, 111520. <https://doi.org/https://doi.org/10.1016/j.oceaneng.2022.111520>

Prabu-Chelladurai, S. K., Dash, A. K., Nagarajan, V., & Sha, O. P. (2023). Longitudinal strength of high block coefficient merchant ships in irregular waves. *Ocean Engineering*, 283, 115066. <https://doi.org/https://doi.org/10.1016/j.oceaneng.2023.115066>

Quispe, J. P., Estefen, S. F., Souza, M. I. L. d., Chujutalli, J. H., Aamante, D. d. A. M., & Gurova, T. (2022). Numerical and experimental analyses of ultimate longitudinal strength of a small-scale hull box girder. *Marine Structures*, 85, 103273. <https://doi.org/https://doi.org/10.1016/j.marstruc.2022.103273>

Shi, G.-J., & Gao, D.-W. (2021). Model experiment of large superstructures' influence on hull girder ultimate strength for cruise ships. *Ocean Engineering*, 222, 108626. <https://doi.org/https://doi.org/10.1016/j.oceaneng.2021.108626>

Song, S., Ehlers, S., Polach, F. v. B. u. p., & Braun, M. (2025). Ultra-low cycle fatigue of ship hull structure: An alternately cyclically loaded four-point bending test of a large box girder. *Marine Structures*, 100, 103732. <https://doi.org/https://doi.org/10.1016/j.marstruc.2024.103732>

Wang, Q., Wang, C., Wu, J., & Wang, D. (2020). Experimental and numerical investigations of the ultimate torsional strength of an ultra large container ship. *Marine Structures*, 70, 102695. <https://doi.org/https://doi.org/10.1016/j.marstruc.2019.102695>

Wang, Q., & Wang, D. (2020). Scaling characteristics of hull girder's ultimate strength and failure behaviors. *Ocean Engineering*, 212, 107595. <https://doi.org/https://doi.org/10.1016/j.oceaneng.2020.107595>

Wang, X., & Gu, X. (2021). Risk-based ultimate strength design criteria for very large floating structure. *Ocean Engineering*, 223, 108627. <https://doi.org/10.1016/j.oceaneng.2021.108627>

Wang, Y., Wei, P., Wang, Q., Dai, Z., & Wang, D. (2024). A new similarity method for the ultimate strength of box girders subjected to the combined load of bending and lateral pressure. *Ocean Engineering*, 313, 119270. <https://doi.org/https://doi.org/10.1016/j.oceaneng.2024.119270>

Wang, Y., Zhang, M., Wei, P., & Wang, D. (2025). Buckling strength driven similarity method for hull girders under combined loads of bending and torsion. *Thin-Walled Structures*, 216, 113689. <https://doi.org/https://doi.org/10.1016/j.tws.2025.113689>

Wang, Z., Kong, X., & Wu, W. (2023). Empirical formula to assess ultimate strength of side shell on passenger ship under combined axial and shear load based on experimental and numerical analysis. *Ocean Engineering*, 288, 116149. <https://doi.org/10.1016/j.oceaneng.2023.116149>

Xu, M. C., Song, Z. J., & Pan, J. (2017). Study on influence of nonlinear finite element method models on ultimate bending moment for hull girder. *Thin-Walled Structures*, 119, 282–295. <https://doi.org/https://doi.org/10.1016/j.tws.2017.06.009>

Yao, T., & Nikolov, P. I. (1992). Progressive collapse analysis of a ship's hull girder under longitudinal bending (2nd report). *Journal of the Society of Naval Architects of Japan*, 172, 437–446. <https://api.semanticscholar.org/CorpusID:113233328>

Zhang, Y., Guo, J., Xu, J., Li, S., & Yang, J. (2021). Study on the unequivalence between stiffness loss and strength loss of damaged hull girder. *Ocean Engineering*, 229, 108986. <https://doi.org/https://doi.org/10.1016/j.oceaneng.2021.108986>

Zhao, N., Wang, Y., Zhang, M., & Guedes Soares, C. (2022). Experimental and numerical investigation on the ultimate strength of a ship hull girder model with deck openings. *Marine Structures*, 83, 103175. <https://doi.org/10.1016/j.marstruc.2022.103175>

Zhu, Z., Ren, H., Incecik, A., Lin, T., Li, C., & Zhou, X. (2024). A novel method for determining the neutral axis position of the asymmetric cross section and its application in the simplified progressive collapse method for damaged ships. *Ocean Engineering*, 301, 117390. <https://doi.org/10.1016/j.oceaneng.2024.117390>